Measurement of Sauter Mean Diameter (SMD) in Diesel Sprays Using a Scattering-Absorption Measurement Ratio (SAMR) Technique

G. L. Martinez[1], F. Poursadegh[1], G. M. Magnotti[1,2] K. E. Matusik[2], D. J. Duke[2], B. W. Knox[1], C. L. Genzale[1], C. F. Powell[2], and A. L. Kastengren[2]

[1]Georgia Institute of Technology – Atlanta, GA

E-mail: gabrielle.martinez@gatech.edu
Telephone: + (714) 271 7373

[2]Argonne National Laboratory – Lemont, IL

Abstract. A new diagnostic for the quantification of Sauter Mean Diameter (SMD) in high-pressure fuel sprays has been recently developed using combined optical and x-ray measurements at the Georgia Institute of Technology and Argonne National Laboratory, respectively. This diagnostic utilizes liquid scattering extinction measurements from diffuse back-illumination imaging, conducted at Georgia Tech, and liquid absorption measurements from x-ray radiography, conducted at Argonne's Advanced Photon Source. The new diagnostic, entitled the Scattering Absorption Measurement Ratio (SAMR), quantifies two-dimensional distributions of path-integrated SMD, enabling construction of the spatial history of drop size development within practical fuel sprays. This technique offers unique benefits over conventional drop-sizing methods in that it can be more robust in optically dense regions of the spray, while also providing high spatial and temporal resolution of the corresponding droplet field.

The methodology for quantification of SMD distributions using the SAMR technique has been previously introduced and demonstrated in diesel sprays using the Engine Combustion Network Spray D injector, however a more detailed treatment of measurement uncertainties has been needed. In the current work, we present a summary of the various sources of measurement uncertainty in the SAMR diagnostic, like those due to the experimental setup, data processing methods, and theoretical assumptions, and assess how these sources of uncertainty affect the quantified SMD. The spatially-resolved SMD measurements that result from the SAMR diagnostic will be especially valuable to the engine modeling community for the quantitative validation of spray submodels in engine CFD codes. Careful evaluation and quantification of measurement uncertainties is important to support accurate model validation and to ensure the development of more predictive spray models.

Notation

SMD	*Sauter Mean Diameter*
I	*Attenuated Light Intensity*
I_o	*Incident Light Intensity*
τ	*Optical Thickness*
PDA	*Phase-Doppler Anemometry*
USAXS	*Ultra-small angle x-ray scattering*
APS	*Advanced Photon Source*
Georgia Institute of Technology	*Georgia Tech*
Argonne National Laboratory	*Argonne*
SAMR	*Scattering Absorption Measurement Ratio*
ECN	*Engine Combustion Network*
DBI	*Diffuse Back Illumination*
$\overline{M}$	*Projected fuel density [$\mu g/mm^2$]*
d	*Droplet size*
LVF	*Liquid volume fraction*
α_{ext}	*Attenuation coefficient*
z	*Illumination path-length*
C_{ext}	*Extinction cross section*
N	*Number of droplets*
FWHM	*Full Width Half Maximum*
NF	*Noise Floor*
λ	*Wavelength of incident light*

1. Introduction

Because the fuel injection process directly controls air-fuel mixing, combustion, and subsequent engine-out emissions in diesel engines, understanding the spray atomization processes is important for the development of efficient and clean diesel engines. Despite recent advances, much remains unknown about the physics governing atomization in high-pressure fuel sprays. Within the literature, several mechanisms have been proposed to explain the primary breakup and atomization process of diesel-type sprays, including internal nozzle flow cavitation, nozzle-generated turbulence, liquid supply oscillations, and growth of aerodynamically-induced interface disturbances [14]. However, to date, direct observation or measurement of the primary breakup and atomization of diesel sprays has not yet sufficiently resolved these processes to identify the relevance of proposed mechanisms with certainty. Execution of direct observation or quantitative measurements of primary breakup and atomization in diesel sprays is challenging due to high number density of the droplet field, small characteristic droplet sizes (~1-20 μm), and high characteristic velocities in the primary breakup region (~600 m/s) [14,15].

Due to the extremely fast time scales encountered, direct observation or imaging of the primary atomization region in diesel sprays is especially difficult. Understanding this process through direct measurement of the formed droplets can be a more feasible approach to understand the atomization process. However, quantitative drop sizing diagnostics can be challenging to employ in diesel sprays due to the high optical thickness of the spray [15]. Phase Doppler anemometry (PDA) is one of the most commonly employed drop sizing diagnostics in spray applications and is useful because droplet size, velocity and volume flux can be measured simultaneously [4]. PDA utilizes two intersecting coherent laser beams to create a small measurement volume for probing individual droplets [4]. The likelihood of multiple droplets existing within the probe volume can become high within high optical thickness sprays, generating a high frequency of invalid measurements [5]. As a result, previous PDA measurements conducted in diesel-like sprays have been limited to locations far downstream of the nozzle [18], far away from the primary breakup and atomization process. Also, because PDA is a pointwise measurement, it can be very time consuming to generate a multi-dimensional scan of the spatial droplet size distribution [4]. In addition, it is often difficult to incorporate the diagnostic in a pressure vessel due to limited optical access [18].

More recently, a new x-ray diagnostic, ultra-small angle x-ray scattering (USAXS), has been applied to diesel sprays to measure droplet sizes [6]. USAXS relies on the high brilliance x-ray beam from the Advanced Photon Source (APS) at Argonne National Laboratory to probe the spray structure [7]. The x-rays are scattered by the electrons in the fuel and the resulting scattering pattern is related to the particle shape and size. Notably, the use of x-rays allows for penetration of the measurement beam through optically thick droplet clouds, enabling the use of USAXS in near-nozzle locations of diesel sprays. Although USAXS provides detailed droplet size information in spray locations that have been previously unattainable, it is a time consuming and resource-intensive diagnostic because each spray measurement location requires a measurement of the scattering signal over a full sweep of scattering angles, resulting in high data throughput requirements. This has limited previous measurements to just a few locations along the spray axis [6]. This diagnostic shows clear advantages in probing high optical thickness sprays, and is thus likely to help advance new knowledge on primary breakup and atomization in diesel sprays. It is limited, however, in its ability to provide a complete spatially resolved picture of the drop size evolution and distribution.

The ideal diagnostic for studying atomization and measuring droplet sizes in high-pressure fuel sprays would: 1) perform under moderate to high optical thickness environments, 2) accurately measure small droplet scales (1-20 μm), 3) provide high temporal resolution, and 4) provide 2D or 3D spatial resolution of the droplet size distribution throughout the spray, supporting a more complete picture of the spray phenomena. Ideally, this diagnostic would also accomplish these goals with a modest level of time and equipment resources. To address these ideals, we have recently developed a new droplet sizing diagnostic, conducted via joint measurements between Georgia Institute of Technology (Georgia Tech) and Argonne National Laboratory (Argonne). This technique is called Scattering-Absorption Measurement Ratio (SAMR) and combines x-ray absorption and visible-light scattering extinction measurements, which are techniques that have been previously employed within diesel sprays at each institution. The ratio of these measurements, combined with Mie-scattering calculations yields 2D volume-projected droplet size distributions in diesel-like sprays within regions of moderate optical thickness [16]. While we have presented an initial demonstration of the new technique in [16], the current work probes further into examining and quantifying measurement uncertainties in the SAMR diagnostic, like those due to the experimental setup, data processing methods, and theoretical assumptions, and assesses how these sources of uncertainty affect the quantified Sauter Mean Diameter (SMD).

2. Experimental Measurements

This paper focuses on two phases of the project. The goal of Phase I was to demonstrate the capability of utilizing these two diagnostics in conjunction to quantify the SMD in optically thin regions of the spray. Comparing data sets acquired from separate experimental facilities requires careful consideration, especially regarding jointly processing the measurements. Therefore, Phase I of the project emphasized the need to establish an appropriate methodology for jointly processing the data sets. The data processing steps will be elaborated upon in Section 3 of the paper. In Phase II, the objective was to refine the experimental aspects of the diagnostic. A different LED was used to evaluate the influence of the wavelength of the light source on the performance of the diagnostic. Also, more careful attention to completely matching the experimental setups of the two facilities was done. A summary of the differences between the two phases of the project is shown in Table 1.

Table 1. Experimental conditions for both phases of the project

	Injector	Light Source	Ambient Density	Nominal Injection Pressure	Section of Paper
Phase I	Spray D #209133	White LED	2.4, 22.8 kg/m^3	50 MPa	4.1 Data Processing Uncertainty Analysis
Phase II	Spray A #306020	Red LED 633 nm	22.8 kg/m^3	50 MPa	4.2 Theoretical Uncertainty Analysis

2.1 Visible Light Scattering Extinction Measurements

Diffuse back-illumination (DBI) experiments were conducted at Georgia Tech in the SPhERe Lab. The SPhERe Lab is equipped with a high-pressure, high-temperature continuous flow spray chamber, which can reach pressures and temperatures up to 100 bar and 900 K, respectively [9]. This spray chamber is optically accessible, which allows for a suite of diagnostics to be employed to directly observe the spray formation process. The spray chamber was designed so that highly characterized engine relevant conditions can be created. This chamber is similar to other continuous flow vessels in the literature [17].

The DBI imaging technique was based on the work by Westlye et al. [22]. The DBI setup creates a diffuse light source to illuminate the spray field. A Photron SA-X2 high speed camera was used to record the intensity of incident and attenuated light. The schematic below shows the experimental setup utilized for the DBI experiments. The LED was pulsed at a rate half that of the camera frame rate. This was intentionally done in accordance with Westlye's recommendations for the DBI diagnostic to reduce the effect of ghosting [22].

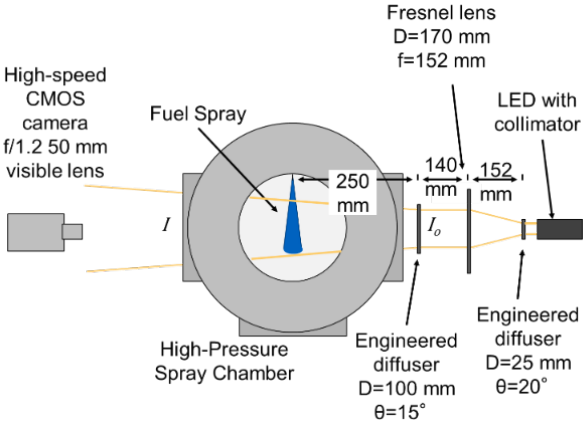

Fig. 1. Diffuse back-illumination experiments were conducted at Georgia Tech using an optical setup which consists of a small engineered diffuser, a Fresnel lens, and a large engineered diffuser as shown above in the schematic

Table 2. Camera and light source settings for both phases of the project

	Camera Lens	Camera Frame Rate	LED pulse rate	Pulse width	Half Collection Angle	Resolution
Phase I	50mm f/1.2	72,000 fps	36,000 fps	90 ns	4.85°	77.7 µm/pixel
Phase II	50mm f/2.8	72,000 fps	36,000 fps	52 ns	4.16°	94.6 µm/pixel

Phase I of this work used the Engine Combustion Network's (ECN) Spray D injector which has a 186 µm nominal outlet diameter, whereas Phase II used the Spray A injector with a 90 µm nominal outlet diameter. Table 1 details the experimental conditions of interest for the two phases of the project. A Bosch common-rail diesel system was used to pressurize the n-dodecane.

DBI was used to measure the optical thickness of a spray. The optical thickness (τ) can be found using the Beer-Lambert law which relates the incident light intensity (I_o) to the attenuated light intensity (I) using the following eq.,

$$\frac{I}{I_o} = e^{-\tau} \tag{1}$$

$$\tau = -\ln(\frac{I}{I_o}) \tag{2}$$

The 2-D line of sight optical thickness maps were developed using this equation. An LED served as the light source for these DBI experiments. The LED illuminated the chamber before the fuel injection began enabling a 2-D measurement of I_o. After the start of injection, the high-speed camera recorded the attenuated light, I, after it passed through the chamber and interacted with the spray [16]. Figure 2 shows the 2-D measured optical thickness maps from the DBI experiments. Figure 2a shows the optical thickness map for Phase I. In this phase, ten injection events were time and ensemble averaged. Figure 2b shows the optical thickness map for Phase II. In this phase, twenty injection events were time and ensemble averaged. This modification to the experimental diagnostic was done in order to improve the signal-to-noise ratio. In addition, for Phase II the data was time averaged from 1.3 to 2.3 ms to match the time averaging window of the radiography data at this condition.

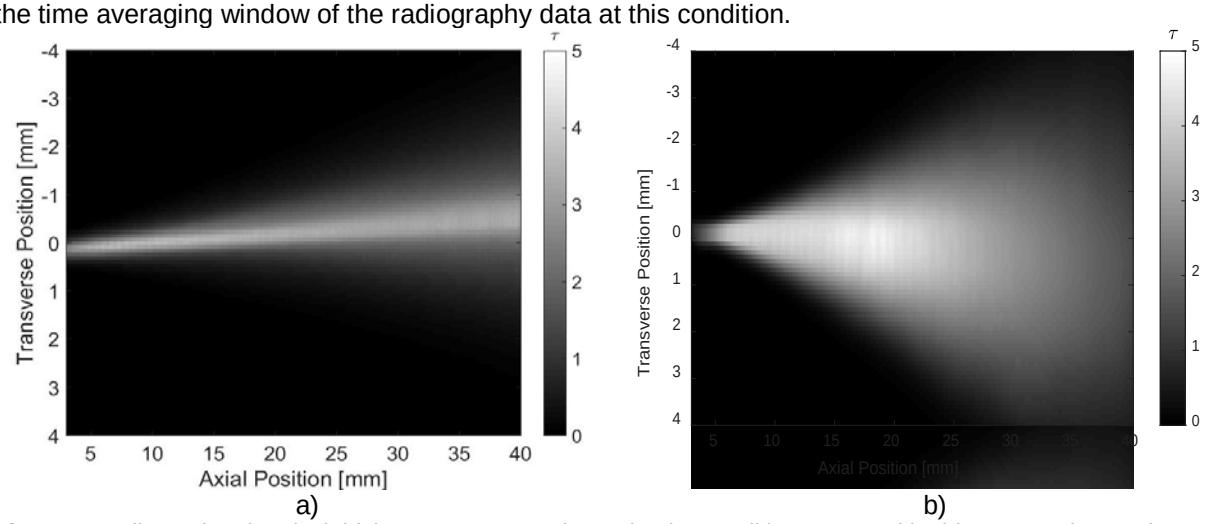

Fig. 2. Two-dimensional optical thickness maps are shown for the conditions covered in this paper. Fig. 2a shows the Spray D 2.4 kg/m^3 50 MPa and Fig. 2b. shows the Spray A 22.8 kg/m^3 50 MPa

2.2 X-Ray Radiography Measurements

Measurements of the time-resolved projected density of the fuel sprays were conducted at the 7-BM beamline of the APS [7]. Each diesel injector was mounted horizontally in a pressure chamber fitted with a pair of x-ray transparent windows. The fuel line was oriented such that it pointed vertically upward, corresponding to the ECN 0° orientation. The chamber was held at room temperature and pressurized with N_2, which was also used to continuously purge the vessel at 4 standard Lmin^{-1} in order to inhibit droplet accumulation within the measurement domain. The working fuel was n-dodecane at room temperature, pressurized by a conventional common-rail diesel system.

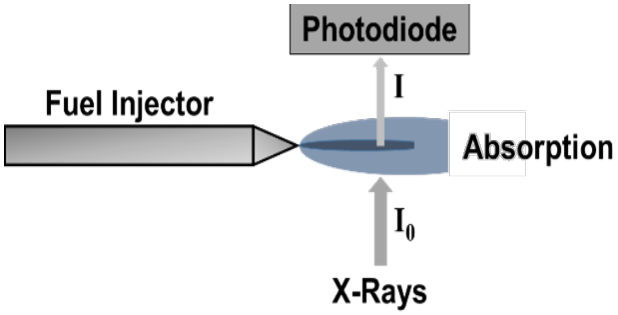

Fig. 3. A schematic of the x-ray radiography setup is shown. The x-ray source is from the Advanced Photon Source at Argonne and the photodiode detects the outgoing x-ray beam intensity

Figure 3 shows a simplified schematic of the experimental diagnostic. A beam of x-rays from the bending magnet source passed through a double crystal monochromator and beam defining slits to create a monochromatic x-ray beam at 8 keV (4.3% bandwidth). The x-rays were focused to a 4μm x 6μm pencil beam with a pair of x-ray focusing mirrors. The incident radiation, I_o, was measured with an intensity monitor before the x-rays impinged on the spray, and the downstream attenuated intensity, I, was recorded at 3.68 μs temporal resolution with a photodiode.

At 8 keV x-ray energy, the main interaction of the photons with the fuel spray is through photoelectric absorption. As the beam passes through the spray, photons are absorbed by the fuel, with the degree of attenuation described by the Beer-Lambert law [1],

$$l = \frac{1}{\mu}\ln\left(\frac{I_o}{I}\right) \tag{3}$$

where l is the effective path length of fuel in units of length, and μ is the linear attenuation coefficient of the fuel, found through calibration. If the fuel density, ρ, is known, the path length, l, can be converted into the projected fuel density, $\bar{M}$ (units μg/mm^2), through the relation,

$$\bar{M} = \rho l \tag{4}$$

In order to build up a 2D map of the fuel spray distribution, the spray chamber was traversed both horizontally and vertically with regard to a fixed beam, and the x-ray intensity was measured at a raster grid of points. To increase the signal-to-noise ratio, between 16 to 32 spray events were averaged at each spatial location.

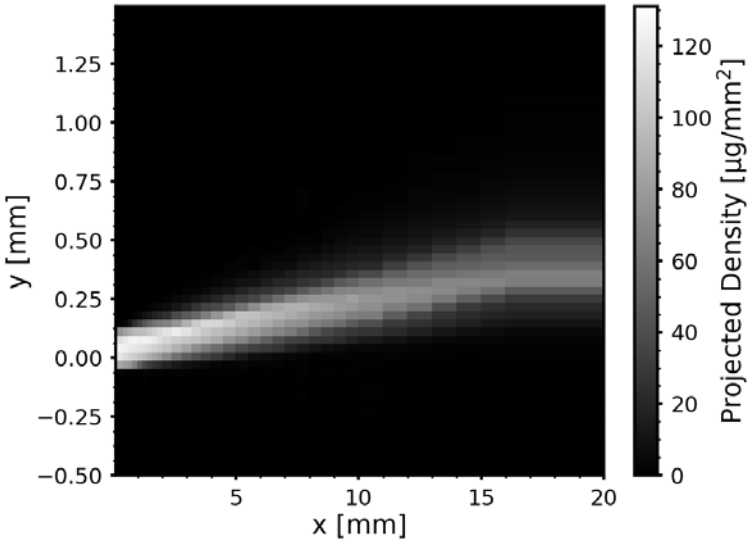

Fig. 4. An ensemble and time averaged two-dimensional map of the projected density is shown for the condition, Spray D 2.4 kg/m^3 50 MPa

3. Scattering Absorption Measurement Ratio (SAMR) Technique

3.1 Theory

The scattering absorption measurement ratio technique has been presented previously in [14, 15, 16]. A summary of the theoretical basis for this measurement ratio will be presented here. The optical thickness, τ, can be related to the droplet size, *d*, liquid volume fraction, *LVF*, when applying Mie's solution to Maxwell's equation [21]. Mie's solution to Maxwell's equations describe the scattering of light by a homogeneous sphere, like a fuel droplet. Firstly, the optical thickness can be related to the attenuation coefficient, α_{ext} and the illumination path-length, *z*.

$$\tau = \alpha_{ext} z \tag{5}$$

The attenuation coefficient can then be re-written in terms of the number weighted extinction cross section, $\overline{C_{ext}}$, where N is the number of droplets in a given volume V

$$\alpha_{ext} = \frac{\overline{C_{ext}} N}{V} \tag{6}$$

For non-absorbing spheres, the extinction cross section equals the scattering cross section. The number of droplets in a given probe volume can be related to the liquid volume fraction.

$$LVF = \frac{V_{liq}}{V} = \frac{\sum_j N_j (\frac{\pi {d_j}^3}{6})}{V} \tag{7}$$

The volume of the droplet can be rewritten as the number weighted mean droplet volume, which allows for further simplification. Finally, the optical thickness can be related to the spray parameters of liquid volume fraction and droplet size.

$$\tau = \frac{\overline{C_{ext}}}{\frac{\overline{\pi d^3}}{6}} * LVF * z \tag{8}$$

For Mie scattering, it is known that the extinction cross section, C_{ext}, is proportional to the cross-sectional area of the droplets [21],

$$C_{ext} \propto d^2 \tag{9}$$

The optical thickness from the DBI experiments can be related to this new expression for optical thickness in the single and independent scattering regime. In optically thin regions of the spray, single scattering can be assumed. For single scattering events, Eq. 2 can be equated to Eq. 8.

Multiple-scattering is a well-recognized source of error in extinction measurement systems utilizing detectors with a finite collection angle [2, 3, 11]. This phenomenon is responsible for redirecting the scattered light back into the detection system, leading to erroneous optical thickness measurements and ultimately an overestimation of local SMD. In Phase II of the project, a multiple scattering correction was employed to reduce some of these errors in optically thick regions of spray (see Section 4.2).

If a measurement of liquid volume fraction were present, the measured droplet size in a given probe volume could be calculated. The projected density, measured from the x-ray radiography measurement, can be recast as liquid volume fraction for non-vaporizing and constant liquid density conditions.

$$\bar{M} = \rho_f \frac{V_{liq}}{V} z \tag{10}$$

Rewriting projected density in terms of liquid volume fraction becomes,

$$\frac{\overline{M}}{\rho_f} = LVF * z \tag{11}$$

Because both of these parameters are functions of liquid volume fraction, taking a ratio of these quantities will yield a relationship to the droplet size. One important consideration in taking this measurement ratio is ensuring that equivalent measurement volumes are being compared. Section 3.2 will elaborate on this point further.

$$\frac{\frac{\bar{M}}{\rho_f}}{\tau} = \frac{LVF * z}{\overline{c_{ext}} * \frac{LVF}{\frac{\overline{\pi d^3}}{6}} * z} \tag{12}$$

Simplifying this expression yields a relationship between our measured quantities (τ and $\bar{M}$) and the mean droplet size within a probed volume or the Sauter Mean Diameter.

$$\frac{\frac{\bar{M}}{\rho_f}}{\tau} = \frac{\frac{\overline{\pi d^3}}{6}}{\overline{c_{ext}}} \alpha \frac{\overline{d^3}}{\overline{d^2}} = SMD \tag{13}$$

The extinction cross section can be found using the publicly available program, MiePlot, [24]. This quantity is proportional to the overall light lost through the scattering process, and here is determined for monodisperse droplet distributions of varying SMD. An illumination wavelength of 633 nm and an index of refraction of 1.422 is considered for fuel droplets (i.e. n-dodecane) in air. The finite collection angle of the extinction setup is also considered to account for the corresponding contribution of the additional light collected through forward scattering. Previous work by Magnotti and Genzale details more of the specifics involved in generating C_{ext} as a function of SMD [14,15]. The calculated C_{ext} is ultimately used to relate SMD to the measurement ratio, as shown in Fig. 5.

The SAMR technique is only valid in the single and independent scattering regime. Optically thin regions of the spray are usually confined to $\tau < 1.0$. It has been shown that errors due to multiple scattering are low for moderate optical thickness levels ($1.0 < \tau < 2.0$) when the measurement involves small collection angles and small droplets [2, 3], which are expected conditions for the SAMR measurements in phase I.

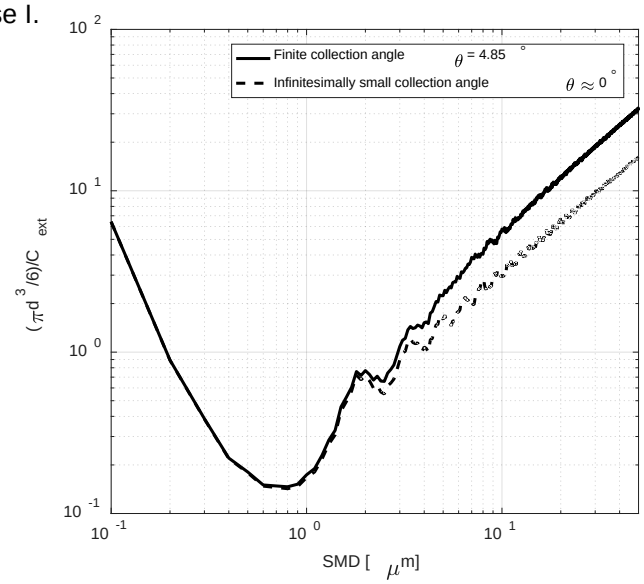

Fig. 5. A graph of the extinction coefficient as a function of the SMD for a finite collection angle and infinitesimally small collection angle [24]

3.2 Joint Processing of Scattering-Absorption Extinction Measurements

Careful consideration is required when comparing data sets from two different experimental facilities. Researchers aimed to keep as much consistent between the two experimental facilities as possible. The ambient densities and injection pressures were closely matched. The injectors were shared between the two laboratories. Commanded injection duration was matched between the setups. Both spatial and rotational alignment of the sprays is important for jointly processing the two measurements. In a previous work, Martinez et al. noticed asymmetries in the spray which may have a large effect on the quantified SMD [16]. For Phase I of the experimental campaign, the orientation between the two facilities was off by about 10°. For Phase II of the project, the injector orientations were matched within approximately 1°. In Section 4.1, the effect of measurement viewing angle on the resulting SMD will be assessed. Alignment in the measurement plane is also important to ensure that equivalent measurement volumes

are being compared. Spatial co-alignment via full width half maximum (FWHM) is currently the method for ensuring that both data sets are aligned in the projected measurement plane. When aligning via this method, the values (optical thickness or projected density) that are equal to half the maximum are found. The center of the spray is defined as the midpoint between the half-maximum values on each side of the projected density and optical thickness distributions. The SAMR results are determined assuming that these two midpoints correspond to the same location in the spray. This is currently the method whereby Argonne aligns the projected density data [8]. The impact of spray misalignment on the SMD will be evaluated later in Section 4.1 of the paper.

Utilizing data sets from two different experimental facilities to extract the SMD requires several processing steps. Some of these processing steps include: co-alignment of the data sets, resampling the data so that measurement resolutions could be matched, curve fitting the projected density, finding an average projected density value, selecting the locations to take a measurement ratio and extracting the Sauter Mean Diameter (SMD).

Figures 6 and 7 illustrate the spatial co-alignment that was performed for the optical thickness and projected density values. Figure 7 shows the importance of spatial co-alignment.

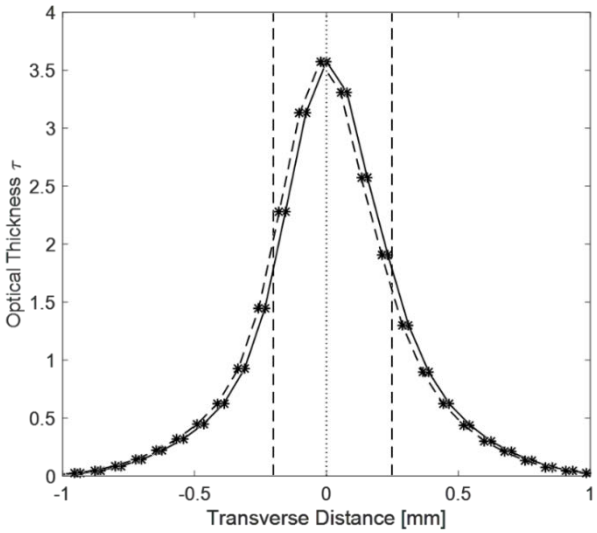

Fig. 6. The transverse profiles of optical thickness are shown for Spray D ρ_{amb}=2.4 kg/m^3 P_{inj}=50 MPa 10 mm away from the nozzle before (solid line) and after (dashed line) shifting via the midpoint between the half maximum

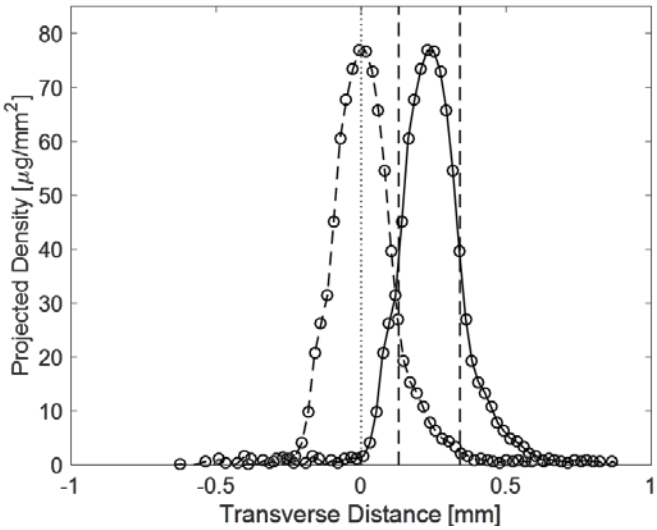

Fig. 7. The transverse profiles of projected density are shown for Spray D ρ_{amb}=2.4 kg/m^3 P_{inj}=50 MPa 10 mm away from the nozzle before (solid line) and after (dashed line) shifting via the midpoint between the half maximum

After the transverse distributions were properly co-aligned, a resampling of the projected density values was necessary. Due to the nature of the radiography measurement (see Section 2.2), it is

possible to achieve finer spatial resolution for the projected density data than the optical thickness data. The resolution of the optical thickness data was limited by the optical setup. To ensure that the joint measurement analysis is conducted for equivalent measurement volumes, a resampling process was established. The resampled measurement volumes or bins are equivalent in size to the spatial resolution of the DBI measurements (see Table 2). Each bin is centered about each optical thickness point. Figure 8 illustrates the optical thickness and projected density values overlaid. The dashed lines on Fig. 8 show the locations of the resampled measurement volumes. The projected density values are also curve fit, shown in Fig. 8. An average from the curve fit is found for each resampled measurement volume.

Another important processing step was identifying the regions where the SAMR measurement is valid without correction for the impact of multiple-scattering. As demonstrated in section 3 in the development of the SAMR theory, the Mie-scatter calculations used to quantify SAMR SMDs are limited to single scattering. When $\tau < 1.0$, single scattering can safely be assumed. However, previous authors [2,3] have indicated that the errors due to multiple scattering are low for $\tau < 2.0$ for diagnostics utilizing small collection angles and measurements of small droplets. Because this is the case for our diagnostic, we have applied the SAMR technique for $\tau < 2.0$.

The measurement validity is constrained by two diagnostic limitations. First, the visible-light extinction signal must not be contaminated by light re-directed into the collection angle by multiple scattering. Second, the noise floor of the radiography measurements limits viable joint measurement regions. As observed in Fig. 8, the optical thickness measurements show a higher sensitivity to detection of liquid in the periphery of the spray compared to the projected density measurements, where the signal decays to the noise floor more rapidly. Combining these two limits, a SAMR measurement ratio can only be accurately quantified for:

a) Single to intermediate scattering regime ($\tau < 2.0$)
b) Projected density > Noise Floor (NF)

For Phase I of the project, both conditions were met. In Fig. 8, the gray shaded boxes indicate the regions where a measurement ratio could be taken. For Phase II of the project, a multiple scattering correction was employed which removed the $\tau < 2.0$ restriction on the utility of the SAMR technique. For this phase, the measurement ratio was only restricted to satisfying b). The theoretical uncertainty analysis of the SAMR diagnostic is presented in Section 4.2.

After the viable regions are identified, a ratio is taken between the average projected density value divided by the fuel density and the optical thickness value (see eqn. 13). This measurement ratio is then related to C_{ext} from MiePlot as shown in Fig. 5. Finally, the SMD can be calculated. Figure 8 below shows most of the aforementioned data processing steps.

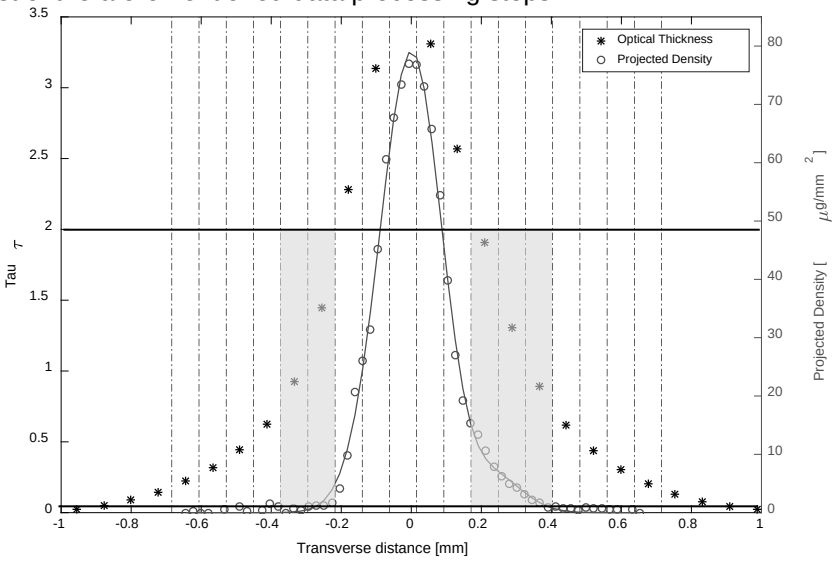

Fig. 8. The optical thickness and projected density values are overlaid for Spray D ρ_{amb}=2.4 kg/m^3 P_{inj}=50 MPa at 10 mm axial location. The dashed lines show the locations of the bins. The projected density values are resampled. An average value is found in each bin from the double Gaussian curve fit, shown in the figure. The gray shaded boxes show regions where the measurement ratio could be accurately interpreted for phase one of the project (before the multiple scattering correction was employed)

4. Uncertainty Analysis

4.1 Data Processing Uncertainty Analysis

Once the data processing steps were established, an uncertainty analysis was done to ascertain the relative effect each processing step had on the quantified SMD. The first processing step that was analyzed was the co-alignment of the data sets. Because the data were taken at two experimental facilities, co-alignment was essential to ensure that the same region of the spray was being analyzed. Additionally,
each facility uses a different coordinate system for the measurements, thus emphasizing the need for spatial co-alignment. This analysis was conducted to determine the sensitivity of the SMD measurement to the translational co-alignment. The DBI and radiography data sets were translated according to FWHM. Next, the projected density values were shifted by distances of 0.05, 0.15, and 0.25 mm in the positive and negative direction. The optical thickness values and the locations of the bins were not changed. The projected density values in each bin do change, which results in a different average projected density value. This new average projected density value is used to calculate a new measurement ratio in that bin, and ultimately, a different SMD. Figure 9 shows the shifting that occurred for the projected density values for Spray D 2.4 kg/m^3 50 MPa at 14 mm axial location.

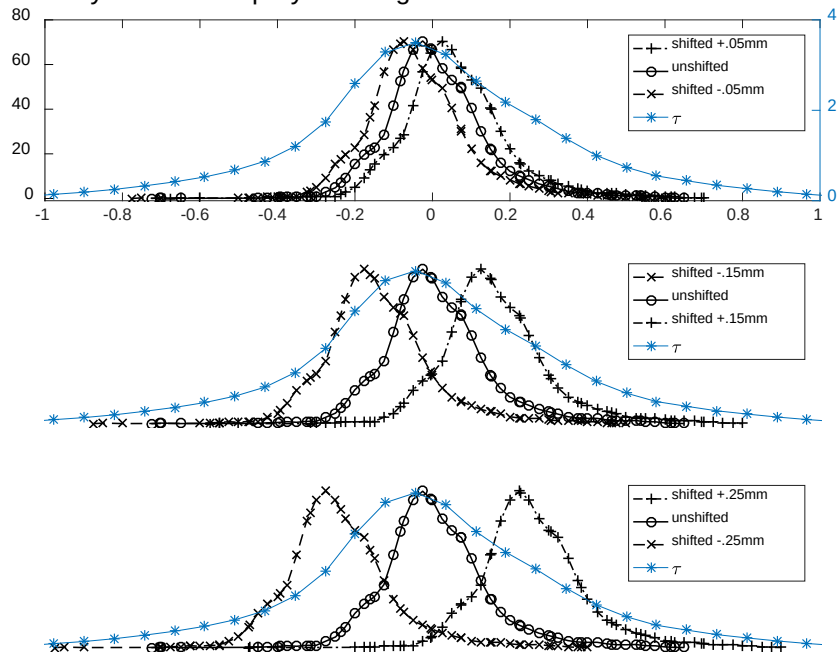

Fig. 9. To assess the importance of the spatial co-alignment of the data sets, we analyzed how the SMD would be affected by shifting the projected density data set by ±0.05 mm, ±0.15 mm, and ±0.25 mm. Condition presented is Spray D ρ_{amb}= 2.4 kg/m^3 P_{inj}=50 MPa at 14 mm away from the nozzle

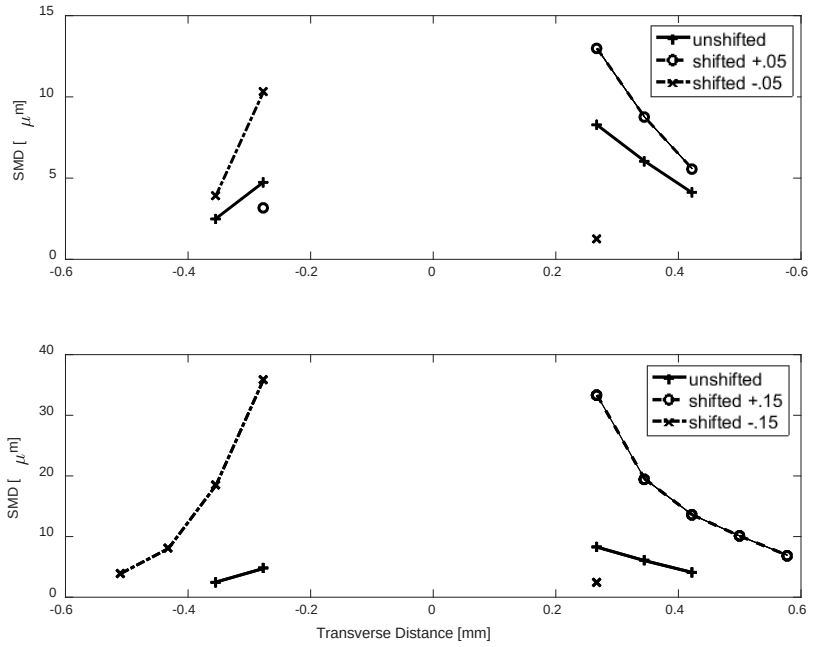

Fig. 10 The SMDs for the original and shifted by ±0.05 mm (top), 0.15 mm (bottom) are shown. Condition presented is Spray D ρ_{amb}= 2.4 kg/m^3 P_{inj}=50 MPa at 14 mm away from the nozzle.

Figure 10 shows the SMDs that are calculated after shifting the projected density values by 0.05 and 0.15 mm, respectively. The SMDs are found only in the optically thin and moderate optical thickness regions of the spray (τ < 2.0). Figure 11 shows the relative error in the quantified SMD for the same conditions shown in Fig. 10. The figures show that that even a relatively small misalignment of the two data sets can have a significant effect on the calculated SMD. Figure 11 indicates that on average the percent difference between the two SMDs is about 30%, but can get as large as 145%. A misalignment of the data sets by up to +/- 0.05 mm could be reasonably judged as “co-aligned” by an observer of the overlapping data sets. Thus, the uncertainty in quantified SMD is highly dependent on the accuracy of co-aligning these data sets. As such, shifting via FWHM seems to reasonably align the datasets and should continue to be used in the future. Increasing the data misalignment by 0.1 mm contributes to an even more substantial error in the measured SMD, resulting in relative errors greater than 100% at all viable measurement locations. Though a misalignment of this magnitude would be more obvious and less likely to be considered as a viable co-alignment of the data sets, these rather large errors indicate how essential it is to carefully consider the spatial alignment of the two data sets from both facilities.

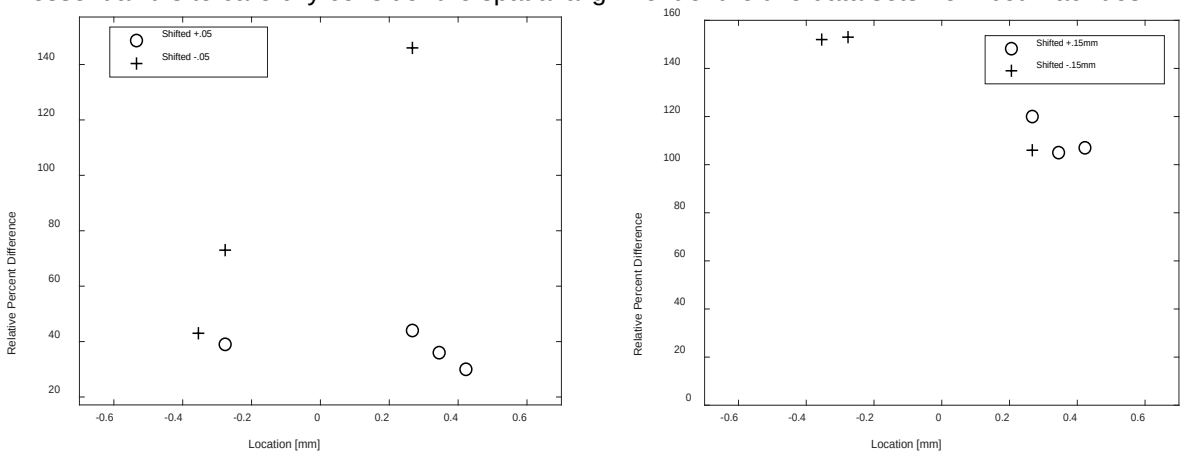

a) b)

Fig. 11. The relative percent differences are shown for the Spray D ρ_{amb}= 2.4 kg/m^3 P_{inj}=50 MPa at 14 mm away from the nozzle for shifting by a) .05 mm and b) .15 mm

The aforementioned uncertainty analysis was also conducted for the Spray D ρ_{amb} = 22.8 kg/m^3 P_{inj} = 50 MPa condition. Figure 12 shows the SMDs for the same condition at an axial location of 14 mm. An interesting trend is shown in Fig. 12. For this higher ambient density case, the SMD values

increase as the distance from the spray centerline increases. This counterintuitive behavior is further discussed in Section 4.2 of the paper. At the 10 mm axial location, the relative percent difference between the FWHM co-aligned measurements and those shifted by ±0.05 mm was 13% and 18%, respectively. For a data set shift of ±.15 mm, the relative difference in SMD was 60% and 68%. Just as with the 2.4 kg/m^3 ambient density case, increasing the spatial misalignment by 0.1 mm increases the percent error significantly.

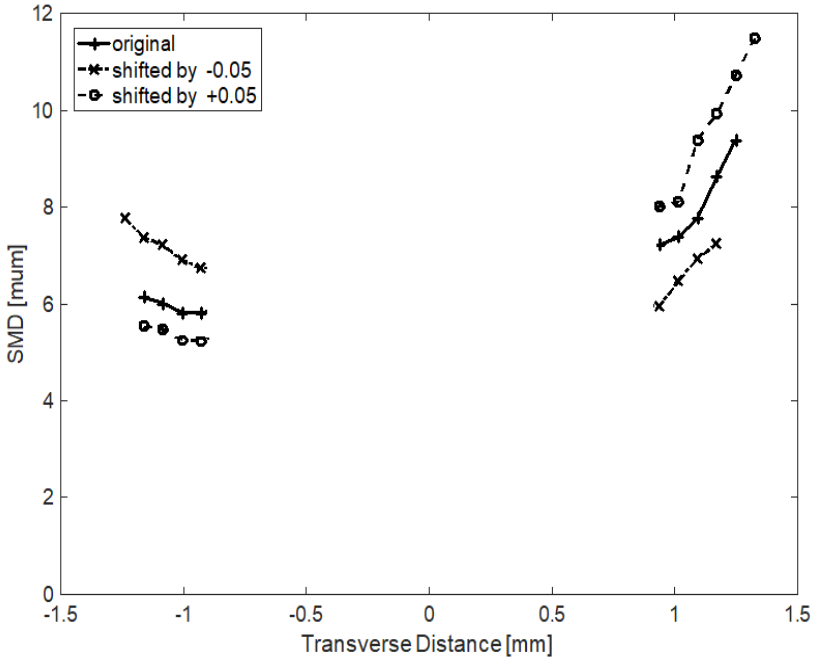

Fig. 12 The SMDs for the original and shifted by ±.05mm are shown. Condition presented is Spray D ρ_{amb}= 22.8 kg/m^3 P_{inj}=50 MPa at 14mm away from the nozzle.

The next portion of the data processing uncertainty analysis consisted of assessing the relative importance of the injector orientation. Previous work by Martinez et al. showed significant asymmetries in the spray thus precipitating a need to assess the importance of the injector orientation. In Phase I, the injector orientation between the two facilities was off by about 10°. This uncertainty analysis enables an assessment of the sensitivity of the SMD measurement to relative differences in facility-to-facility injector orientation. This analysis consisted of processing the projected density with 0° and 180° orientations. The orientation of the optical thickness values was not changed. While flipping the data sets by 180° may not capture all the possible asymmetries in the spray, it allowed for an analysis of the importance of the injector orientation between the two facilities. Figure 13 shows the transverse profiles of the projected density for 0° and 180° orientations with the optical thickness overlaid.

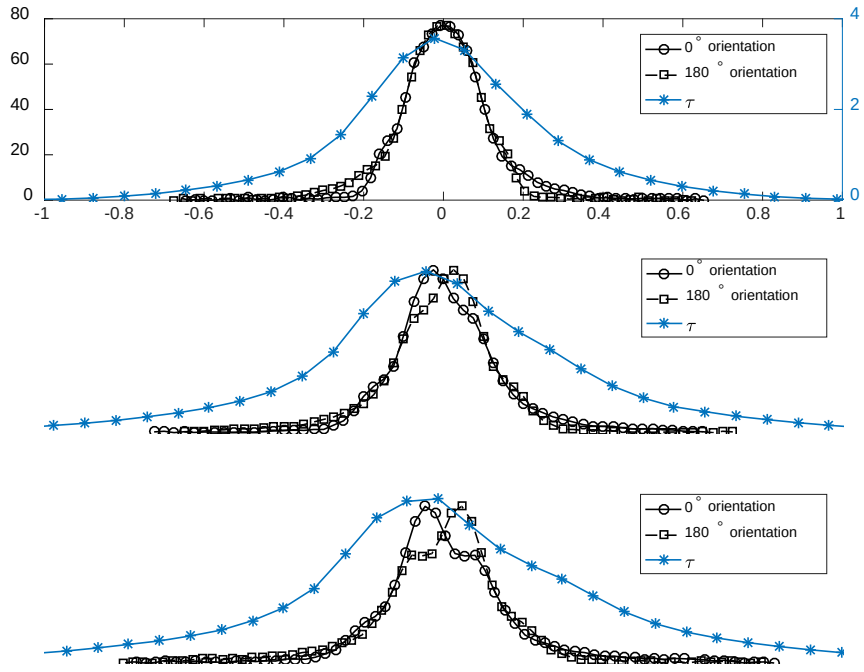

Fig. 13 To assess the importance of the rotational alignment of the data sets, the projected density values were analyzed for 0° and 180° orientations. These figures are displaying the condition Spray D ρ_{amb}= 2.4 kg/m^3 P_{inj}=50 MPa at 10, 14, 16 mm axial locations (from top to bottom) respectively

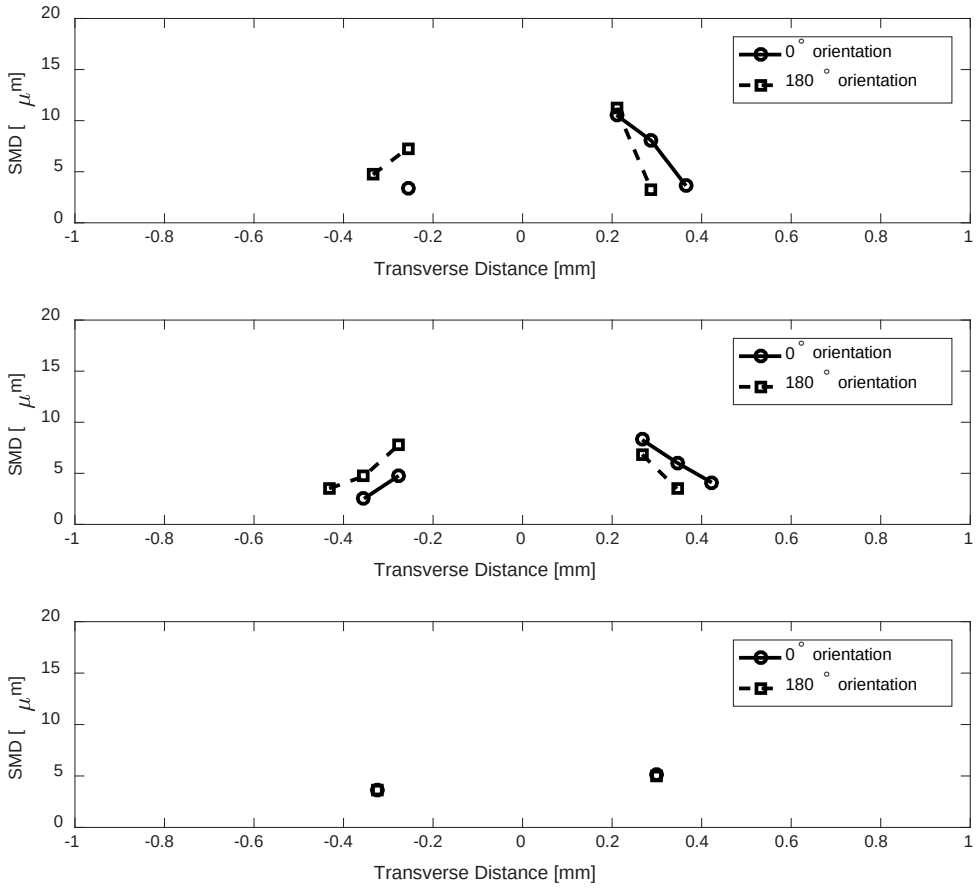

Fig. 14. The SMDs are shown for the 10, 14, 16 mm axial locations for Spray D 2.4 kg/m^3 and 50 MPa for the 0° and 180° orientations

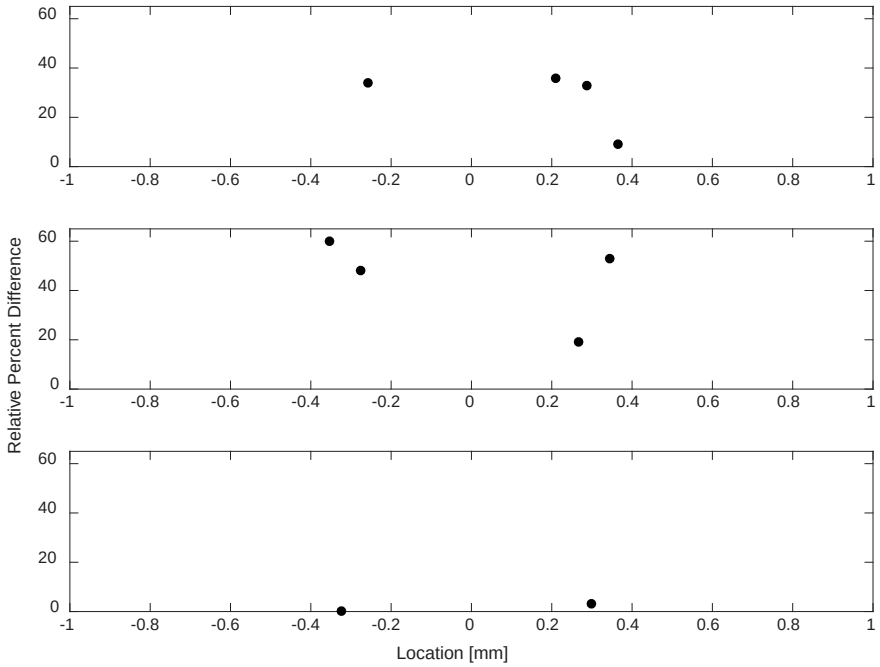

Fig. 15. The relative percent differences for the 0° and 180° orientations are shown. Condition presented is Spray D ρ_{amb}= 2.4 kg/m^3 P_{inj}=50 MPa at 10, 14, 16 mm away from the nozzle

Figure 13 illustrates the asymmetries present in the spray, as illustrated by the "shoulders" in the projected density values. The projected density values do not decrease to zero at the same rate, indicating an additional asymmetry. This asymmetry in slope of the projected density measurements relative to the change in optical thickness is one of the driving factors in relative percent differences for both shifting the data and changing the spray orientations. When the data is processed for both injector orientations, the measurement ratio and the SMD are affected. Figure 14 shows the SMD values for both injector orientations. For the 10 and 14 mm axial locations, the maximum difference in the droplet size is 3 μm. The high ambient density condition (22.8 kg/m^3) also shows a difference in the SMD of about 3 μm. At 16 mm away from the nozzle exit, the maximum difference in the droplet size is only 0.2 μm. Figure 15 demonstrates that the relative error between the two injector orientations ranges from less than 1% up to 60%. Overall, this rotational alignment uncertainty analysis indicates the importance of matching the injector orientation. In Phase II of this work, the injector orientation for both facilities was matched to minimize error due to rotational misalignment.

4.2 Theoretical Uncertainty Analysis

A theoretical uncertainty analysis was conducted on the data taken during the second phase of the project. As discussed earlier, multiple scattering may have a significant impact on the extinction measurement in a system with a finite collection angle. Therefore, it is crucial to quantify and account for the contribution of multiple-scattering to the measured optical thickness in order to achieve an accurate SMD estimation using the proposed method. Correcting for the multiple scattering effect will also allow for a measurement ratio to be taken everywhere throughout the spray. This will provide a better understanding of the SMD field. To correct for multiple scattering, the modification proposed by Berrocal et al. is first adapted to the current optical system and then used to correct the measured optical thickness [2,3].

According to Berrocal [2], the measured optical thickness (τ_{meas}) can be corrected (τ_{corr}) using the following expression to account for the influence of multiply scattered light. Note that the corrected optical thickness represents that for a system with infinitesimally small collection angle.

$$\tau_{meas} = \tau_{corr} - \alpha\, \tau_{corr}^{\beta}\,, \tag{14}$$

where the coefficients α and β are related to the collection angle of the detection system and size of droplets present in the probe volume. Berrocal et al. reported the values of these coefficients for the two collection angles of 3.3° and 10.3° (i.e. recalculated in a manner consistent with the current work) and mono-disperse particle sizes ranging from 1 to 20 μm, illuminated by a near infrared light source emitting at a wavelength of 800 nm [2, 3]. Hence, these constants are first linearly interpolated to match the

collection angle of the current detection system stated in Table 1, and then adopted to account for the difference in the wavelength of incident light. According to the theory of light scattering, particles of identical size parameter demonstrate the same scattering behavior. The size parameter x is defined as

$$x = \frac{\pi d}{\lambda}, \tag{15}$$

where d is the size of particles/droplets and λ is the wavelength of the incident light. Equation 15 can be used to find the size of droplets exhibiting similar scattering behavior at 633 nm to those reported in the literature, d_{Lit}, illuminated at 800 nm [2, 3]

$$d_{633} = \frac{633}{800}\, d_{Lit}, \tag{16}$$

Equations 14 and 16 are then used to construct a transfer function for correcting the measured optical thickness using the current system. The correction process requires a knowledge of both the measured optical thickness and local droplet size. While the former is directly measured through the extinction setup, the latter is initially an unknown parameter. Therefore, the implementation of Eq. 15 involves an iterative process, where the constructed transfer function is coupled to Eq. 14 and solved iteratively to compute the actual optical thickness of the spray field and the corresponding SMD.

Figure 17 illustrates the contribution of multiple scattering on the measured optical thickness for the Spray A 22.8 kg/m^3 and 50MPa at three axial locations from the nozzle. This phenomenon has a significant impact on the DBI measurement along the injector axis where the optical thickness is the highest. The multiple scattering effect, however, becomes less severe and eventually negligible towards the periphery of the spray, where the corresponding optical thickness approaches zero. This trend is expected largely due to the dominance of low-order scattering events in this region. The multiple scattering correction was only employed in the regions where this phenomenon may be of considerable impact (i.e. τ> 1). The corresponding SMD distributions are shown in Fig. 17. An average SMD of 6 µm is measured along the spray centerline. While the distribution of SMD remains fairly uniform for a large proportion of the spray width, it sharply rises at the peripheral region of the spray. This is particularly the case farther downstream of the injector at 16 mm axial location. This trend is consistent with earlier observations in the literature [12, 18, 20, 23]. This counterintuitive increase in SMD at the spray periphery is primarily attributed to two potential mechanisms: droplet collision/coalescence at the peripheral region due to shear effects [23], and transport of large droplets from the core region due to vortex effects at the spray tip [10].

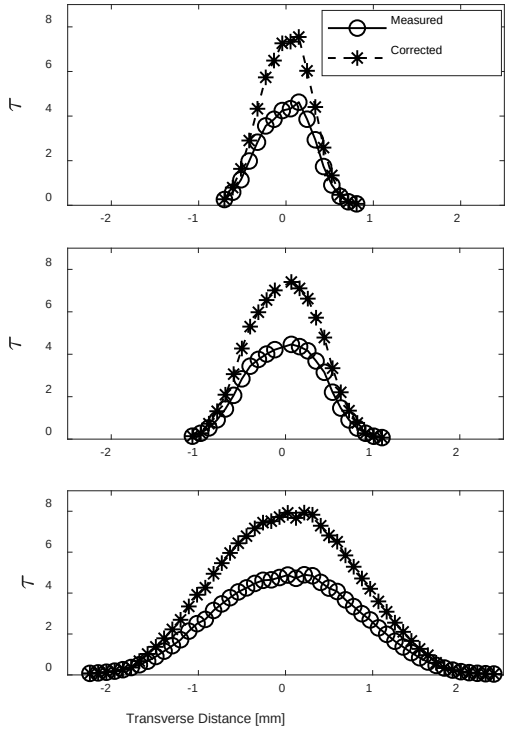

Fig. 16 The radial distribution of measured and corrected optical thickness for the Spray A 22.8 kg/m^3 50 MPa condition at axial locations of 8, 10 and 16 mm (from top to bottom respectively).

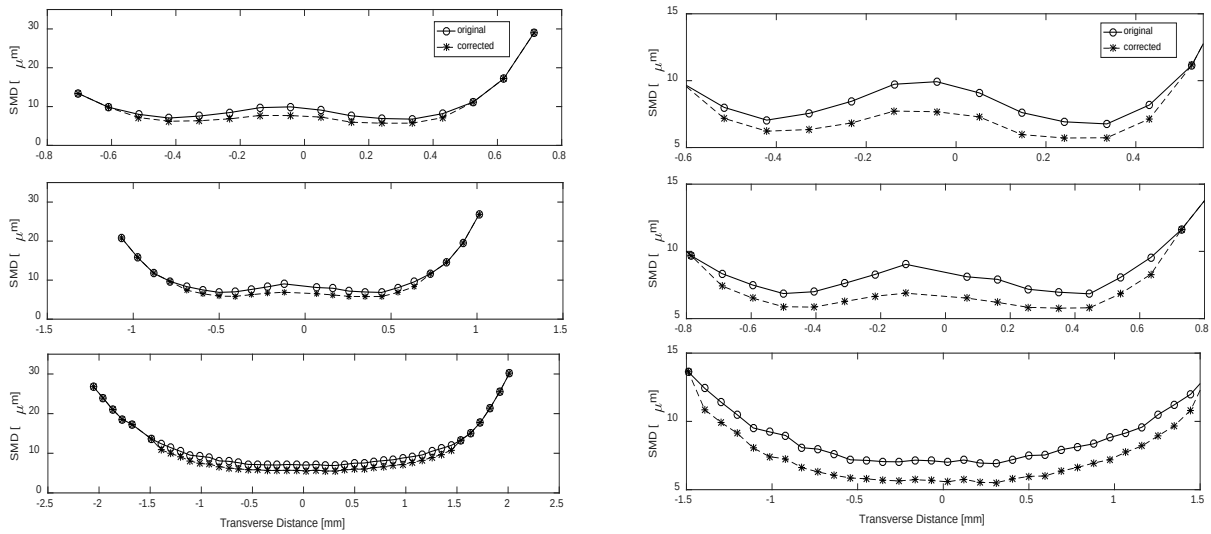

Fig. 17 The radial distribution of measured and corrected SMDs are shown for the Spray A 22.8 kg/m^3 50 MPa condition axial locations of 8, 10 and 16 mm (from top to bottom respectively). Figure 17a shows all of the corrected and original SMD values, whereas Fig. 17b shows a detailed view to illustrate the discrepancies in SMD.

Figure 17 shows the SMDs calculated using the measured and corrected optical thickness values. At the periphery of the spray where $\tau < 1$ and single scattering events are assumed, the multiple scattering correction was not applied, so the SMDs for the original and corrected values overlap. Figure 17b shows a detailed view at the regions where the multiple scattering correction was applied. In these regions, the uncorrected results overestimate the size of droplets by a maximum of about 2 μm. This is attributed to the contribution of multiple scattering phenomenon, which results in an underestimation of the local optical thickness (as shown in Fig. 16) and hence an overestimation of the corresponding droplet sizes.

One source of uncertainty in the multiple scattering correction is that the transfer function for correcting the measured optical thickness was interpolated between 5 and 15 μm. To minimize such uncertainties, the authors are planning to construct an empirical transfer function for the range of plausible particle/droplet sizes, which can then be used to confidently correct the extinction measurements in the entire spray field, and therefore have a more accurate prediction of local SMD values.

5. Conclusions and Future Work

This work summarized and probed the accuracy of a recently proposed spray diagnostic for the measurement of droplet sizes in high-pressure fuel sprays, the Scattering-Absorption Measurement Ratio. SAMR utilizes diffuse back illumination measurements of optical thickness from Georgia Tech and spray radiography measurements of projected liquid density from Argonne National Laboratory. Taking a ratio of these two measurements, in combination with application of Mie-scattering theory, produces a measurement of the 2D volume-projected Sauter Mean Diameter. Jointly processing the two experimental measurements from two different facilities involved spatial and rotational alignment of the data sets, resampling the projected density data to co-align the measurement volumes, finding an average projected density within each measurement volume, and taking a ratio between the projected density and optical thickness. Each of these processing steps can introduce error and uncertainty into the final SMD and the influence of these steps was quantified in terms of measurement uncertainty.

The measurement uncertainty introduced by steps required to co-align the Georgia Tech and Argonne data sets was examined by assessing the impacts of spatial and rotational co-alignment on the quantified SMD. It was determined that misalignment of the data sets by 0.05 mm resulted in an uncertainty in the quantified SMD of about 30-70%, thus indicating the necessity of data co-alignment via FWHM method. The effect of relative rotational alignment or measurement viewing angle was also analyzed by comparing the SMDs calculated from projected density measurements orientated at viewing angles of 0° and 180°. This level of rotational misalignment between the two data sets produced an uncertainty in the quantified SMD of less than 1% and up to 60%. Thus, measurement errors due to either rotational or translational misalignment of the spray coordinate systems are of similar magnitude

and can produce SMD measurement uncertainties of up to 60-70%. Further steps should be taken experimentally to minimize these co-alignment uncertainties to improve the accuracy of the SAMR measurement.

A theoretical assumption of single-scattering in the DBI measurement is necessary to quantify SMD from the SAMR. Measurements taken outside of the single and intermediate scattering regime ($\tau > 2.0$) were previously removed from consideration when calculating the SMD. In the current work, a correction equation available in the literature was used to estimate the adverse impact of multiple scattering. Using this correction, the uncertainty in measured SMD within these regions was estimated rather than discarding the data. Within the most optically dense regions of the spray along the spray centerline, multiple scattering is estimated to contribute to an uncertainty of about 1-2 μm in the measured SMD, or a relative error of 10-20%. In other words, the estimated uncertainty in the measured SMD due to multiple scattering is actually lower than those associated with the co-alignment of data sets from the two different measurement facilities.

Future work will seek to minimize the uncertainties in the SAMR technique by addressing the injector orientation uncertainty and correcting for the impact of multiple scattering. A radiography experimental campaign was conducted in which measurements were taken at six viewing angles. The DBI experiments will also be conducted with multiple viewing angles. This will give more information about the asymmetries present in the spray. The multiple scattering correction can also be improved by developing a more accurate transfer function for this experimental setup. This will be instructive in understanding the SMD trends in the radial and axial directions. Ultimately, a two-dimensional SMD map can be created to better understand the evolution of the spray field.

Acknowledgements

This material is based upon work supported by the Department of Energy, Office of Energy Efficiency and Renewable Energy (EERE) and the Department of Defense, Tank and Automotive Research, Development, and Engineering Center (TARDEC), under Award Number DE-EE0007333. X-ray measurements were performed at the 7BM and 9ID beamlines of the Advanced Photon Source, an Office of Science User Facility operated for the U.S. Department of Energy (DOE) Office of Science by Argonne National Laboratory, and supported by the U.S. DOE under Contract No. DE-AC02-06CH11357.

References

[1] Als-Nielsen, J. and McMorrow, D. Elements of Modern X-ray Physics. 2nd Edition. John Wiley & Sons, West Sussex, United Kingdom, 2011.

[2] Berrocal, E. “Multiple scattering of light in optical diagnostics of dense sprays and other complex turbid media” PhD Dissertation, School of Engineering, 2006

[3] Berrocal, E., Sedarsky, D. L., Paciaroni, M. E., Meglinski, I. V. and Linne, M. A. “Laser light scattering in turbid media Part I: Experimental and simulated results for the spatial intensity distribution” *Optics express,* Optical Society of America, 2007, 15, 10649-10665

[4] Fansler, Todd D., Parrish, Scott E., “Spray measurement technology: a review” *Measurement Science and Technology*, 2015.

[5] Jermy, M. C. and Greenhalgh, D. A. “Planar dropsizing by elastic and fluorescence scattering in sprays too dense for phase Doppler measurement” Applied Physics B. Volume 71, pages 703-710, 2000.

[6] Kastengren, Alan L. Ilavsky, J, Viera, Juan Pablo, Payri, Raul, Duke, D. J., Swantek, Andrew, Tilocco, F. Zak, Sovis, N., Powell, Christopher F., “Measurements of droplet size in shear-driven atomization using ultra-small angle x-ray scattering” International Journal of Multiphase Flow, Volume 92, 2017, Pages 131-139.

[7] Kastengren, A. L., Powell, C.F., Arms, D., Dufresne, E.M., Gibson, H., and Wang, J. (2012) The 7BM beamline at the APS: a facility for time-resolved fluid dynamics measurements. *J. Synch. Rad.* 19: 654-657.

[8] Kastengren, A. L., Powell, C.F., Wang, Y., Im, K. S., and Wang, J. “X-ray radiography measurements of diesel spray structure at engine-like ambient density” *Atomization and Sprays* 19, no. 11, 2009.

[9] Knox, B. W. “End of Injection Effects on Diesel Spray Combustion” PhD Dissertation, Georgia Institute of Technology, 2016.

[10] Kosaka, H., Suzuki, T., and Kamimoto, T. “Numerical simulation of turbulent dispersion of fuel droplets in an unsteady spray via discrete vortex method” 1995, SAE Technical Paper (No. 952433).

[11] Labs, J. E., Parker, T., “Multiple-scattering effects on infrared scattering measurements used to characterize droplet size and volume fraction distributions in diesel sprays” *Applied optics, Optical Society of America,* 2005*, 44*, 6049-6057

[12] Labs, J. E., Parker, T., “Diesel fuel spray droplet sizes and volume fractions from the region 25mm below the orifice.” *Atomization and Sprays*, vol. 13, pp. 45-62, 2003.

[13] Lefebvre A. H., *Atomization and Sprays*, New York, Taylor and Francis, 1989.

[14] Magnotti, Gina M., “Modeling the influence of nozzle-generated turbulence on diesel sprays,” PhD Dissertation, Georgia Institute of Technology, 2017.

[15] Magnotti, Gina M., and Genzale, Caroline L., “Detailed assessment of diesel spray atomization models using visible and X-ray extinction measurements,” *International Journal of Multiphase Flow*, 97:33-45, 2017.

[16] Martinez, Gabrielle L., Magnotti, G. M., Knox, B. W., Matusik, K. E., Duke, D. J., Kastengren, A. L., Powell, C. F., and Genzale C. L. “Quantification of Sauter mean diameter in diesel sprays using scattering-absorption extinction measurements.” ILASS-Americas 29th Annual Conference, Atlanta, GA, May 2017.

[17] Meijer, Maarten, Bart Somers, Jaclyn Johnson, Jeffrey Naber, Seong-Young Lee, Louis Marie Malbec, Gilles Bruneaux et al. "Engine Combustion Network (ECN): Characterization and comparison of boundary conditions for different combustion vessels." *Atomization and Sprays* 22, no. 9 (2012).

[18] Payri, R., Araneo, L., Shakal, J., & Soare, V. “Phase doppler measurements: system set-up optimization for characterization of a diesel nozzle”. *Journal of mechanical science and technology*, 2008, *22*(8), 1620-1632.

[19] Reitz, Rolf D., Bracco, F. “Mechanisms of breakup of round liquid jets,” *Encyclopedia of fluid mechanics*, vol. 3, pp. 233–249, 1986.

[20] Smallwood, G. J., Gulder O. L., “Views on the structure of transient diesel sprays”. Atomization and Sprays. 2000, 10(3-5), pp 355-386.

[21] Van de Hulst, H. C. *Light Scattering by Small Particles,* Dover Publications, 1981.

[22] Westlye, F.R., Penney, K., Ivarsson, A., Pickett, L., Manin, J., and Skeen, S. “Diffuse back-illumination setup for high temporally resolved extinction imaging.” Applied Optics, 2017.

[23] Wu, K. J., Reitz, R. D., and Bracco, F. V. “Measurements of drop size at the spray edge near the nozzle in atomizing liquid jets”. *Physics of fluids*, 1986 *29*(4), 941-951.

[24] http://www.philiplaven.com/mieplot.htm, accessed January 2018.